Journal of Drug Metabolism and Toxicology

Ryosuek Takahashi, Akiko Hisada, J Drug Metab Toxicol 2013, 4:2
DOI: 10.4172/2157-7609.1000146

Research Article Open Access

Higher Expressions of Cytochrome P450, UDP-Glucuronosyltransferase, and Transporter Genes in Nanopillar-Cultured Rat Hepatocyte Spheroids

Ryosuke Takahashi*, Akiko Hisada and Hiroshi Sonoda

Advanced Research Department, Central Research Laboratory, Hitachi, Ltd. Hatoyama, Saitama 350-0395, Japan

Abstract

Primary hepatocytes have been widely explored as cell sources for the study of *in vitro* drug metabolism and pharmacokinetics (DMPK). Aiming toward establishing an *in vitro* drug screening method, the objective of the current study is to illustrate a comprehensive increase in the DMPK-related gene expression of nanopillar (NP)-cultured 3D-spheroids. To examine the expressional changes in DMPK-related genes under four different conditions, namely, NP-, sandwich (SW)-, monolayer (ML)-cultured rat hepatocytes, and freshly isolated hepatocytes, genome-wide gene-expression analysis using a DNA microarray was performed. Among the DMPK-related genes, cytochrome P450, UDP-glucuronosyltransferase, and transporter genes were focused on. Principal component analysis showed that the global gene expression profile in a sample from an NP culture was closer to that from freshly isolated hepatocytes than to that from an SW culture. The expressions of almost all Cyp 1 to 3 and Ugt genes of NP-cultured 3-D spheroids were higher than those of ML and SW. The expression of the Abcc2 gene, whose translation product has a critical role in the excretion of metabolized bile acids in hepatocyte to bile canaliculi, was three times higher in NP than in ML. From these results, 3-D spheroids formed by the NP culture were suggested to possess a higher ability of metabolism and excretion than does 2-D tissue formed by the conventional monolayer culture.

Keywords: Hepatocyte spheroids; Transporter genes; Bioavailability

Abbreviations: DMPK: Drug Metabolism and Pharmacokinetics; NP: Nanopillar; SW: Sandwich; ML: Monolayer; Cyp: Cytochrome P450; 3-D: Three Dimensional; 2-D: Two Dimensional; Ugt: UDP-Glucuronosyltransferase; Abcc: ATP-binding cassette transporter superfamily C member 2; MRP2: Multidrug resistance-associated protein 2; ADME: Absorption, Distribution, Metabolism and Excretion; ECM: Extracellular Matrix; PCR: Polymerase Chain Reaction; CDFDA: 5-carboxy-2', 7'-dichlorofluorescein diacetate; Cy3: Cyanine 3; DTT: Dithiothreitol; FDR: False Discovery Rate; HCA: Hierarchical Clustering Analysis; PCA: Principal Component Analysis; Slco: Solute carrier organic anion transporter; HMG-CoA: Hydroxymethylglutaryl-CoA

Introduction

In the preclinical stage of drug discovery, evaluating drug metabolism and pharmacokinetics (DMPK) is essential [1]. To determine the DMPK properties of drug candidates, it is necessary to evaluate the process of absorption, distribution, metabolism, and excretion (ADME) within the body [1]. Most of these evaluations are currently performed using a whole animal [2]. Unfortunately, only a small fraction (~10%) of drug candidates that were selected for clinical development eventually have become marketed drugs in recent years [3,4]. The failure rate of drugs in clinical trials could be attributed to poor DMPK and low bioavailability [1]. This situation explains the fact that animal study may not be sufficient for predicting the fate of drug candidates in humans [3]. Accordingly, there is a growing need for a high-throughput *in vitro* method for evaluating DMPK properties that can extrapolate to human very early in the drug discovery process. This makes a contribution to reduction of the attrition during development instead of using the conventional *in vivo* preclinical test that uses animals [5]. Suitable DMPK features of a drug are essential in regard to the reliable selection of effective drug candidates in the clinical development stage and successful progression of those candidates without attrition through clinical evaluation [1].

To date, primary hepatocytes have been extensively used as a cell source for studying *in vitro* drug metabolism and excretion. Hepatocytes in their native environment possess a structural polarity and liver-specific functions such as drug metabolizing or albumin secretion [6,7]. Conventionally cultured hepatocytes have spreading-monolayer morphology on an extracellular matrix (ECM)-coated culture surface [8-10]. The intrinsic differentiated structure and function of hepatocytes rapidly deteriorate or are lost and cannot be recovered under such monolayer culture conditions [6,11]. Accordingly, this 2-D monolayer culture system has difficulty in predicting such a metabolic process as DMPK in all native environments. This difficulty is one of the potential limiting factors in establishing an *in vitro* assay system.

In comparison, 3-D hepatocyte spheroids sustain viability for extended culture periods and higher liver-specific functions [6,12-16]. A spheroid culture system is thus an alternative culture technique for evaluating drug metabolism in the course of drug screening [2,11]. The authors previously developed culture devices for forming 3-D spheroids, namely, nanopillar (NP) sheets, and reported that the spheroid formation of rat primary hepatocytes was controlled by optimizing the pillar diameters and pillar pitch (pillar center-to-center distance) of the NP sheets [13]. In the report, the NP-cultured spheroids possessed higher viability and polarity, and liver-specific functions related to metabolism and excretion were also induced by overlaying Matrigel on the spheroids. These hepatocellular functions

***Corresponding author:** Ryosuke Takahashi, Advanced Research Department, Central Research Laboratory, Hitachi, Ltd., Hatoyama, Saitama 350-0395, Japan, Tel: +81-49-296-6111; Fax: +81-49-296-5999; E-mail: ryosuke.takahashi.jr@hitachi.com

Received January 28, 2013; **Accepted** March 23, 2013; **Published** March 25, 2013

Citation: Ryosuek Takahashi, Akiko Hisada, Hiroshi Sonoda (2013) Higher Expressions of Cytochrome P450, UDP-Glucuronosyltransferase, and Transporter Genes in Nanopillar-Cultured Rat Hepatocyte Spheroids. J Drug Metab Toxicol 4: 146. doi:10.4172/2157-7609.1000146

were assessed by using a gene-expression analysis of the Cyp3a23/3a1 and Abcc2 genes with a real-time polymerase chain reaction (PCR) and by using a 5-carboxy-2', 7'-dichlorofluorescein diacetate (CDFDA) excretion assay. In addition, the NP sheet has an advantage in that it can be used to set up more reproducible culture conditions because its surface geometry can be designed artificially [13]. These advantages of the NP culture will contribute to acquiring stable and reproducible preclinical data and establishing an alternative culturing technique for evaluating metabolism and toxicity in future drug screening processes.

Toward establishing an *in vitro* drug screening method that reflects a drug's DMPK properties within the body, the objective of the current study is to elucidate that the expression levels of cytochrome P450, UDP-glucuronosyltransferase, and transporter genes are higher overall in the NP-cultured 3D spheroids than in the conventional 2-D tissue. Taking particular note of these DMPK-related genes, we therefore performed a genome-wide gene-expression analysis by using a DNA microarray to assess the gene expression profiles of four different conditions, namely, NP, sandwich (SW), and monolayer (ML) cultures and freshly isolated hepatocytes. The DNA microarray analysis could show an entire image of the gene expression profile that cannot be read in the real-time PCR that focuses on individual genes. Moreover, pathway analysis based on the altered gene expression reveals the expressional dynamics. In this report, we describe the 3-D spheroids formed by the NP culture possess a higher ability of metabolism and excretion than does 2-D tissue formed by the conventional monolayer culture. The result suggests that the NP culture is valuable for evaluating metabolism and toxicity toward new drug development.

Materials and Methods

NP sheet preparation

Preparation of the NP sheet was described in the previous report [13]. In brief, a 1.0-mm-thick polystyrene film was spin-coated onto a glass substrate. A nanomold was made of silicon wafer and fabricated by photolithography. The NP sheets (with a 2.0-μm pillar diameter and with pitches twice the pillar diameter) were formed by pressing the mold onto the film at 423 K and then releasing it at room temperature. The NP sheets were precoated with a solution containing 100 ng/ml of type-I collagen.

Hepatocyte culture

Hepatocytes were isolated from six- to eight-week-old specific viral-pathogen-free male Fisher rats weighing about 150–250 g (Charles River Japan Inc., Japan) by modified two-step *in situ* collagenase perfusion [17] and purified by Percoll gradient separation [18]. The viability of the hepatocytes was determined by trypan blue exclusion, and hepatocytes with over 85% viability were used for the following culture.

The hepatocytes were resuspended in William's E medium containing 10% fetal bovine serum supplemented with 8.6 nM of insulin (Sigma-Aldrich Corp., MO), 255 nM of dexamethasone (Nacalai Tesque, Inc., Japan), 50 ng/ml of epidermal growth factor (Sigma-Aldrich Corp.), and 5 KIU/ml of aprotinin (Wako Pure Chemical Industries, Ltd., Japan). The cells were seeded at a density of 1×10^5 cells/cm^2 onto prepared NP sheets or into a 35-mm-diameter culture dish (AGC Techno Glass Co., Ltd., Japan) in which type-I collagen was pre-coated. The seeded hepatocytes were incubated in a humidified chamber with 5% CO_2 at 37°C. The procedure for the NP, SW, and ML cultures is described below.

NP culture [13]: after 24 hours of post-seeding, the medium was replaced with serum-free William's E medium containing the same supplements described above. After 48 hours of post-seeding, the medium was replaced with a serum-free medium containing Matrigel™ (BD Bioscience, MA) with the same supplements described above. Subsequently, the culture medium was changed daily. Hepatocytes were cultured in total for 96 hours.

SW culture [19,20]: after 24 hours of post-seeding, the culture medium was replaced with serum-free William's E medium containing Matrigel (BD) with the same supplements described above. Subsequently, the culture medium without Matrigel was changed daily. Hepatocytes were cultured in total for 96 hours.

ML culture: the culture medium was replaced with serum-free William's E medium every 24 hours. Hepatocytes were cultured in total for 96 hours.

DNA microarray analysis

Total RNA was extracted from the four kinds of samples mentioned above by using an RNeasy Plus Micro Kit (Qiagen GmbH, Germany) according to the manufacturer's instructions. The quantity and quality of the RNA were determined with a Nanodrop ND-1000 spectrophotometer (Thermo Fisher Scientific Inc., Waltham, MA) and an Agilent Bioanalyzer (Agilent Technologies, Palo Alto, CA), as recommended.

Total RNA was amplified and labeled with Cyanine 3 (Cy3) by using an Agilent Low Input Quick Amp Labeling Kit, one-color (Agilent Technologies, Palo Alto, CA) following the manufacturer's instructions. Briefly, 100 ng of total RNA was reverse-transcribed to double-strand cDNA by using a poly dT-T7 promoter primer. The primer, template RNA, and quality-control transcripts of the known concentration and quality were first denatured at 65°C for 10 min and incubated for two hours at 40°C with 5X first-strand buffer, 0.1-M DTT, 10-mM dNTP mix, and Affinity Script RNase Block Mix. The Affinity Script enzyme was inactivated at 70°C for 15 min. cDNA products were then used as templates for *in vitro* transcription to generate fluorescent cRNA. The cDNA products were mixed with a transcription master mix in the presence of T7 RNA polymerase and Cy3 labeled-CTP and incubated at 40°C for two hours. The labeled cRNAs were purified by using Qiagen's RNeasy mini spin columns and eluted in 30 μl of nuclease-free water. Subsequently, the amplified cRNA quantity and labeled cyanine incorporation were determined by using the Nanodrop ND-1000 spectrophotometer and the Agilent bioanalyzer [21]. 1.65 μg of Cy3-labeled cRNA was fragmented and hybridized at 65°C for 17 hours to an Agilent Whole Rat Genome Microarrays 4×44 K (Design ID: 014879). Finally, microarrays were scanned by using an Agilent DNA microarray scanner.

The microarray data were analyzed by using an GeneSpring GX 10.0.2. (Agilent Technologies) at DNA Chip Research Inc. (Kanagawa, Japan). The raw microarray data are available in the GEOarchive file format in the Gene Expression Omnibus with accession number GSE38950 at http://www.ncbi.nlm.gov/geo/. The intensity values of each scanned feature were quantified by using an Agilent Feature Extraction Software version 10.5.1.1, which performs background subtractions. Only features that were flagged as not errors (present flags) were used, and features that were not positive, not significant, not uniform, not above the background, saturated, and population outliers (marginal and absent flags) were excluded. Normalization was performed by using the Agilent GeneSpring GX version 10.0.2. (per

chip: normalization to 75-percentile shift; per gene: normalization to median of all samples) [21]. There are a total of 41,012 probes on the Agilent Whole Rat Genome Microarray 4×44 K (Design ID: 014879), and there are no control probes. Data filtration was performed, and we eventually acquired a valid 22,596 probe set, where at least four out of a total of twelve samples had had the present flag for further analysis. The altered transcripts were quantified by using the comparative method. To identify significant differences in gene expression between samples, False Discovery Rate (FDR)-corrected p-value <=0.01 combined with >=2 to 10-fold change in signal intensity was applied in this study. Hierarchical clustering analysis (HCA) [22] and principal component analysis (PCA) [23] were performed by using the GeneSpring GX 10.0.2.

Gene expression data were mapped to rat pathways of GenMAPP 2.1, and MAPPFinder 2.0 was used to find significant pathways in which a relative amount of genes satisfy the following several-fold-change criteria: 4.0 < [ML/NP] < 8.0, 2.0 < [ML/NP] < 4.0, -4.0 < [ML/NP] < -2.0, -8.0 < [ML/NP] < -4.0, 4.0 < [SW/NP] < 8.0, 2.0 < [SW/NP] < 4.0, -4.0 < [SW/NP] < -2.0, and -8.0 < [SW/NP] < -4.0.

Results

Tissue morphology under three different culture conditions: NP, SW, and ML cultures

Rat primary hepatocytes were cultured to compare tissue morphologies produced under three different culture conditions, namely, NP, SW, and conventional ML cultures. Phase-contrast micrographs of the cultures at 96 hours of post-seeding are shown in figure 1. Spheroids with diameters of 50 to 100 μm and a compact morphology in which individual cells can barely be distinguished on the NP sheet were observed (Figure 1a). Clear bile canaliculi were observed at cell-cell adhesion sites in the SW culture, meaning that each cell had a higher structural polarity (Figure 1b, arrow heads). Individual cells strongly adhered to the substrate and spread in the ML culture (Figure. 1c).

Determination of individual variability by hierarchical clustering analysis (HCA)

To investigate the expressional change of DMPK-related genes in these three kinds of cultured tissue and freshly isolated hepatocytes that resemble native liver parenchymal cells, DNA microarray analysis was conducted. To visualize possible similarities and differences between gene expression profiles, hierarchical clustering analysis (HCA) was performed after whole genome gene expression profiles of four groups were generated by using the Agilent Whole Rat Genome Microarrays 4×44 K. Hierarchical clustering of gene expressional data is an intuitive way to analyze the expressional trends of differentially expressed genes and the relationships between different groups of gene expression patterns. HCA of all 22,596 probes was performed by using the GeneSpring software to examine the similarity of gene expressional profiles of four groups, namely, NP, SW, ML cultures and freshly isolated hepatocytes. The number of samples in each group was three, which are from three different rats (biological replicates). A hierarchical cluster diagram of these 12 samples (freshly isolated hepatocytes -1, -2, and -3; ML-1, -2, and -3; SW-1, -2, and -3; and NP-1, -2, and -3) based on the HCA results is shown in figure 2. The diagram showed that the 12 samples were divided into four clusters according to the four groups. This result indicates that the individual variability in each expressional profile was little. NP and SW belonged to the same cluster by clustering with higher hierarchy. This result means that the expression profile of the NP culture is related more closely to that of the SW culture that was reported to reflect the native environment rather than to that of the ML culture. The freshly isolated hepatocytes had longer clustering distances to all the other groups.

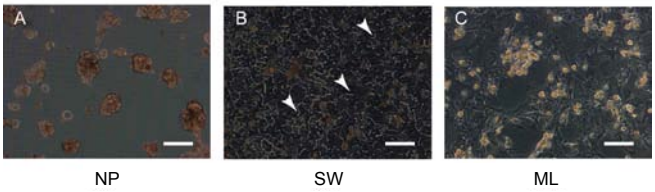

Figure 1: Phase-contrast micrographs of (a) nanopillar (NP)-, (b) sandwich (SW)-, and (c) monolayer (ML)-cultured hepatocytes. Micrographs were taken at 96-h postseeding. Scale bars: 100 μm.

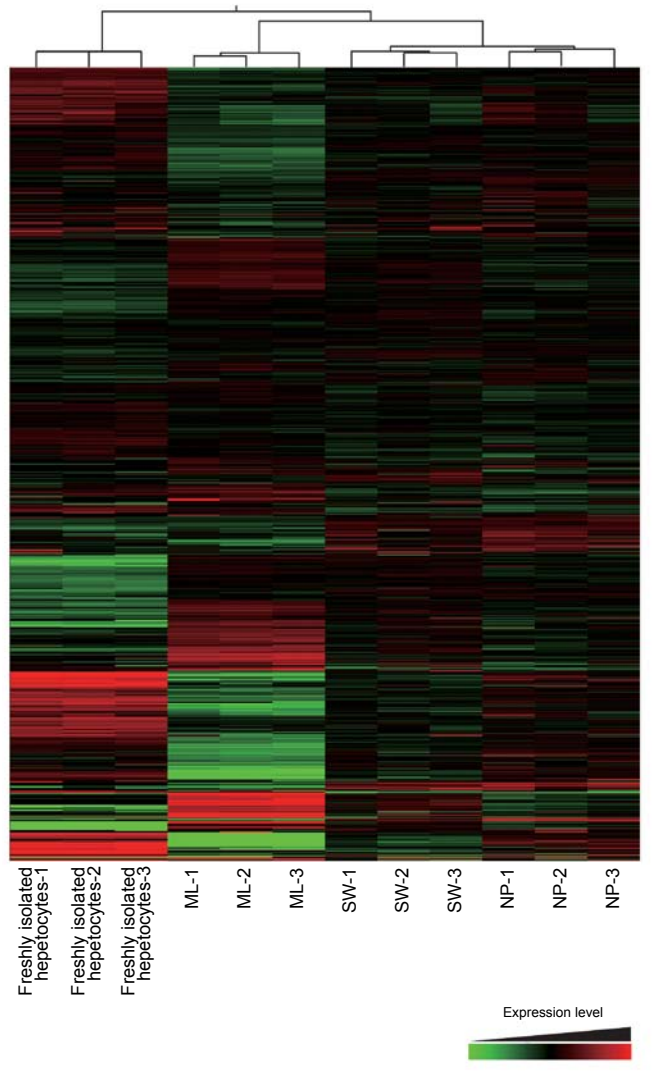

Figure 2: Hierarchical clustering analysis of gene expression of freshly isolated hepatocytes-1, -2, and -3, ML-1, -2, and -3, SW-1, -2, and -3, and NP-1, -2, and -3. The clustering is based on all the 22,596 probes that passed quality filtering. Data were subjected to HCA by using a Euclidian-distance calculation based on the centroid-linkage rule.

Close association between NP and freshly isolated hepatocytes investigated by principal component analysis (PCA)

The similarity and differences between the genome-wide gene expressions of the NP, SW, and ML cultures and freshly isolated hepatocytes (the number of samples in each group is three of biological replicates) were further investigated by principal component analysis (PCA). PCA allows correlations in datasets to be visualized by compressing information in a low number of dimensions. The method is very flexible, and large datasets can be handled easily. An important step in PCA is determining the number of latent variables, which contain relevant information [23]. PCA with all 22,596 probe sets was performed by using the Gene Spring software. The three most variable principal components (PC1, PC2, and PC3) are plotted in three dimensions in figure 3. In the graph, freshly isolated hepatocytes and ML are plotted widely apart, and NP and SW are plotted closely between freshly isolated hepatocytes and ML in PC1 (63.3%). NP is plotted slightly closer to the freshly isolated hepatocytes than is SW in PC1, which means that the expressional profile of NP is more similar to that of the freshly isolated hepatocytes than that of SW. NP and SW are plotted closely, as well as the freshly isolated hepatocytes and ML, in PC2 (26.8%). However, these two groups are plotted widely apart in PC2, respectively.

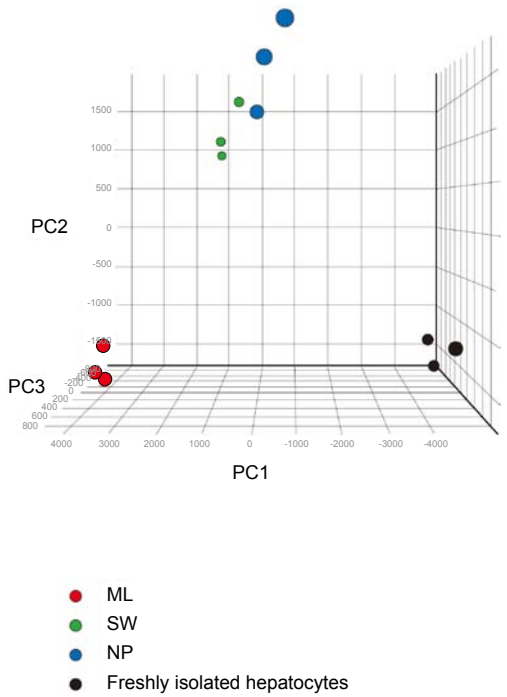

Figure 3: Principal component analysis of gene expression of freshly isolated hepatocytes-1, -2, and -3, ML-1, -2, and -3, SW-1, -2, and -3, and NP-1, -2, and -3. For the 22,596 probes that passed quality filtering, the relative contribution of the variance is shown by three major principal components plotted in three dimensions.

Higher hepatocellular functions related to drug metabolism and excretion in the NP-cultured 3-D spheroid

To assess the expressional changes of DMPK-related genes under four different conditions, the genes of the following three kinds were analyzed: (1) cytochrome P450s (Cyps), which encode a ubiquitous superfamily of heme-containing monooxygenase enzymes that plays a fundamental role in the metabolism of chemically diverse compounds such as endogenous chemicals and pharmaceutical agents [24], (2) UDP-glucuronosyltransferases (Ugts), which encode catalyze enzymes whose role is to add a glycosyl group from a UTP-sugar to a small hydrophobic molecule [25], and (3) solute-carrier organic anion transporters (Slcos) and an ATP-binding cassette transporters superfamily C (Abccs), which encode uptake and excretion transporters, respectively [26]. The expressional ratios of NP/ML, NP/SW, and NP/freshly isolated hepatocytes are represented from top down for each gene in figure 4. In the case that the expression level in the denominator is higher than that in the numerator, the expressional ratio will converge at 0 to 1. To avoid the graphs becoming illegible, the horizontal axis in figure 4 is the exponent.

First, the gene expressions of Cyps were analyzed (Table 1). The translation products of Cyps, which are called "phase I metabolic enzymes", metabolize approximately 70% of drugs in clinical use, and these Cyps belong to Cyp families 1 to 3 [27]. In this case, of the valid results for 66 genes belonging to all Cyp families, the results of 14 genes belonging to Cyp 1 to 3 out are described (Figure 4). The results showed that the Cyps expression level of NP was higher than that of ML in all 12 genes. Furthermore, that of NP was higher than that of SW in the 10 genes not including Cyp1a2 and 2j4. These results mean that the Cyps expression level of the 3-D NP culture was higher than that of a conventional 2-D culture such as SW and ML, which indicates that the 3-D NP culture exhibited better performance closer to an *in vivo* environment than did the conventional 2-D culture. When the NP culture was compared with freshly isolated hepatocytes, the expression levels of Cyp1a1 and 3a1 in the NP culture were significantly higher.

Next, the gene expressions of Ugts were analyzed (Table 1). The translation products, which are called "phase II metabolic enzymes", metabolize about 30-40% of drugs in clinical use [27], and these expressions were analyzed. As a result, the expression level of the NP was higher than that of ML and SW in all genes except for Ugt1a2 (Figure 4). This result indicates that the expression levels of the phase II genes were increased more in the 3-D spheroid by the NP culture than in the 2-D tissue by the conventional ML culture. The expression level of Ugt1a1, one of the key conjugation enzymes whose substrate is a bilirubin, was the highest in the NP culture in all four conditions. Sulfotransferases (Sults) and glutathione S-transferases (Gsts) are also predominant phase II metabolic enzymes. In the present study we investigated the Sult1c1 and Ste (Sult1e1) genes as Sult genes, and Gstm1 (glutathione S-transferase M1) as Gst gene. The expressions of Sult1c1 and Ste in NP-cultured 3-D spheroids were both higher than those in monolayered ML and SW although they were less than freshly isolated hepatocytes (Figure 4). The expression of Gstm1 was increased more in the NP-cultured 3-D spheroid than in the 2-D tissues by the conventional ML and SW cultures. As a result, the expressions of genes not only Ugts but also Sults and Gsts in NP-cultured 3-D spheroids were higher than those in monolayered ML and SW.

Third, the expressions of transporter genes whose translation products have the significant role of taking substrate into hepatocyte and excreting bile acid or metabolites into bile canaliculi were analyzed (Table 1). As in the current pre-clinical *in vivo* trials using animals, quantitative assessment of uptake and excretion will be predominant, which will be similar for *in vitro* assays using cells in the future [28]. A number of uptake transporters are expressed on the hepatocellular membrane. In particular, OATPs that are the translation products of Slco genes perform a crucial role in the uptake of bile acids or one of the primary pharmaceutical agents of HMG-CoA reductase inhibitor such

Probe name	Accession ID	Gene symbol	Major GO term biological process
A_43_P15534	NM_017111	Slco1a1	GO:0006811(ion transport)
A_42_P708480	NM_131906	Slco1a4	GO:0006811(ion transport)
A_44_P203532	NM_131906	Slco1a4	GO:0006811(ion transport)
A_44_P113879	NM_030838	Slco1a5	GO:0006811(ion transport)
A_44_P320677	NM_130736	Slco1a6	GO:0006811(ion transport)
A_44_P328097	NM_031650	Slco1b2	GO:0006811(ion transport)
A_44_P373483	NM_022667	Slco2a1	GO:0006810(transport)
A_44_P491450	NM_080786	Slco2b1	GO:0006810(transport)
A_44_P128007	NM_080786	Slco2b1	GO:0006810(transport)
A_44_P337125	NM_133608	Slco4a1	GO:0006810(transport)
A_44_P321009	NM_012540	Cyp1a1	GO:0006118(electron transport)
A_44_P142025	NM_012541	Cyp1a2	GO:0006118(electron transport)
A_42_P654578	NM_012692	Cyp2a1	GO:0006118(electron transport)
A_44_P356143	NM_012693	Cyp2a2	GO:0006118(electron transport)
A_44_P316194	NM_017156	Cyp2b15	GO:0006118(electron transport)
A_44_P205599	NM_173294	Cyp2b3	GO:0006118(electron transport)
A_44_P280786	NM_019184	Cyp2c	GO:0006118(electron transport).
A_43_P13939	NM_017158	Cyp2c7	GO:0006118(electron transport)
A_44_P327817	NM_138514	Cyp2c13	GO:0006118(electron transport)
A_44_P325666	NM_012730	Cyp2d26	GO:0006118(electron transport)
A_44_P409232	NM_031543	Cyp2e1	GO:0006118(electron transport)
A_42_P678870	NM_019303	Cyp2f2	GO:0006118(electron transport)
A_42_P792497	NM_023025	Cyp2j4	GO:0006118(electron transport)
A_42_P785801	NM_173144	Cyp3a1	GO:0006118(electron transport)
A_44_P147020	NM_001044770	Cyp4a11	GO:0006118(electron transport)
A_43_P12051	NM_019623	Cyp4f2	GO:0006118(electron transport)
A_44_P446578	NM_012683	Ugt1a1	GO:0006789(bilirubin conjugation)
A_44_P432355	NM_201423	Ugt1a2	GO:0008152(metabolic process)
A_44_P402641	NM_201423	Ugt1a2	GO:0008152(metabolic process)
A_44_P432358	NM_057105	Ugt1a6	GO:0006805(xenobiotic metabolic process)
A_44_P247784	NM_153314	Ugt2b3	GO:0006805(xenobiotic metabolic process)
A_44_P236068	NM_001004271	Ugt2b4	GO:0008152(metabolic process)
A_42_P670179	NM_001007264	Ugt2b5	GO:0008152(metabolic process)
A_44_P405190	NM_031732	Sult1c1	GO:0006790(sulfur metabolic process)
A_44_P359759	NM_012883	Ste	GO:0008202(steroid metabolic process)
A_43_P11776	NM_017014	Gstm1	GO:0008152(metabolic process)
A_44_P252417	NM_022281	Abcc1	GO:0006810(transport)
A_43_P11580	NM_012833	Abcc2	GO:0006810(transport)
A_44_P344679	NM_133411	Abcc4	GO:0006811(ion transport)
A_44_P257526	NM_133411	Abcc4	GO:0006811(ion transport)
A_42_P568172	NM_053924	Abcc5	GO:0006810(transport)
A_42_P463998	NM_031013	Abcc6	GO:0006200(ATP catabolic process)
A_43_P11674	NM_013039	Abcc8	GO:0005975(carbohydrate metabolic process)
A_44_P455479	NM_013040	Abcc9	GO:0006810(transport)
A_44_P219628	NM_053840	Ggt1	GO:0006520(amino acid metabolic process)
A_44_P385117	NM_001005889	Rdx	GO:0045176(apical protein localization)

Table 1: Genes investigated in this study.

as pravastatin, pitavastatin, atorvastatin, and fluvastatin [29]. Then, we analyzed the expressions of the Slco genes. The result showed that the expression level of almost all the Slco transporter genes from the 3-D NP culture tended to be higher than that from the conventional 2-D ML or SW cultures (Figure 4). In contrast, the expression levels of all the Slco genes investigated in this study from the NP culture were lower than that from freshly isolated hepatocytes (Figure 4). This result indicates that establishing an *in vitro* culture system that reconstructs the expression level of uptake transporter genes similar to the native liver is difficult even if the formation of 3-D tissue by the NP culture was achieved. From the viewpoint of drug metabolism, Slco1a1 is a key molecule whose substrates are bile acids and the cholesterol-lowering pravastatin [30]. The expression level of this gene extracted from the 3-D NP culture was 24 times higher than that from the 2-D ML culture (Figure 4). Although the absolute values of expressional ratios determined by the current microarray analysis are different from those determined by previous real-time PCR analysis (data not shown), the expressional trend of Slco1a1 was reproduced. The expression trend of Abcc genes is different for each individual gene. The expression of Abcc2, whose main function is to excrete glucuronidated bilirubin to bile acid [31,32], and that of Abcc6, whose function is unknown so far [33], were both higher in the NP-cultured 3-D spheroid than in the ML-cultured 2-D tissue. In contrast, the expression of Abcc1, whose function is to excrete glutathione conjugate or leukotriene

[34,35], and that of Abcc5, whose main function is to excrete cyclic nucleotide [36], were both higher in the ML-cultured 2-D tissue than in the NP-cultured 3-D spheroid (Figure 4). Abcc2 plays a significant role in the excretion of metabolized bile acids in hepatocyte to bile canaliculi, and this is the gene that we have ever been focusing on. We previously reported that the gene expression level of the Abcc2 gene in the NP-cultured 3-D spheroid was determined to be about five times higher than in the ML-cultured 2-D tissue by using real-time PCR analysis [13]. In comparison, it was three times higher according to the results of the present study using microarray analysis. As a result, the 3-D spheroid culture using the NP sheet was endorsed to be a more effective method for Abcc2 expression. Furthermore, we specified gamma-glutamyltransferase 1 (Ggt1) whose molecular function is gamma-glutamyl transpeptidase (γGTP) activity, which is the major enzyme in liver [37,38]. γGTP is present in the cell membranes of many tissues, including the bile duct, and involved in amino acids transfer and metabolism. This means γGTP is the primary indicator of hepatic function such as biliary excretion that we have been focusing on. Although we could not obtain the data of freshly isolated hepatocyte, the expression of Ggt1 in cells cultured by NP was higher than that by monolayer and sandwich. This is the important finding to upgrade the value of the NP culture.

Pathway analyses were introduced to characterize the expressional profile obtained under different culture conditions (Table 2). In order to investigate the metabolic ability of 3-D spheroids formed by the NP sheet, we focused on the Irinotecan pathway (http://www.pharmgkb.org/pathway/PA2001). As a result, the pathway was more activated in the NP-cultured 3-D spheroids than in the ML- or SW-cultured 2-D tissue under the assumed criterion of -4.0 < [ML/NP] < -2.0 and -4.0 < [SW/NP] < -2.0. The dynamics of ADME-related molecules in liver cells such as Oatps, Cyps, Ugts, and Abccs, which are the molecules we specified in this study, are depicted in this Irinotecan pathway and are also involved in the pharmacokinetics of other common drugs and xenobiotics. The result indicates that 3-D spheroids formed by the NP culture possessed higher metabolic ability than did those formed by the conventional 2-D monolayer culture.

Finally, we investigated the correlation between tissue structure and gene expressions. We previously reported that decreased expression of cell-matrix adhesion-related gene such as talin correlates with the increased hepatic function such as upregulation of Abcc2 gene by way of 3-D structure formation [13]. Then, we examined the pathway related to cell-matrix adhesions. As a result, Actin Cytoskeleton and Alpha6-Beta4-integrin pathways were both found to be more activated in the ML-cultured tissue than in the NP-cultured one under the assumed criterion of 2.0 < [ML/NP] < 4.0. In a similar fashion, Alpha6-Beta4-integrin and Focal Adhesion pathways were both found to be more activated in the SW-cultured tissue than in the NP-cultured one under the assumed criterion of 2.0 < [SW/NP] < 4.0. These results mean that the pathway related to cell-matrix adhesion is more activated in the ML- or SW-cultured 2-D cultures than in the NP-cultured 3-D spheroids. In relation to tissue structure, hepatocellular polarity is also one of the primary factor that fulfill the hepatocellular function. Then, we focused on the expression of radixin, the dominant ERM protein. As a result, the NP-cultured 3-D spherood was higher than that in ML- and SW-cultured monolayer tissue (Figure 4). This result means that the structure of NP-cultured spheroid is better organized than the conventional 2-D culture.

Discussion

The Agilent Whole Rat Genome Microarray was used to comprehensively examine the hepatocellular functions related to DMPK and compare the expressional profiles obtained from the 3-D NP culture with those from the 2-D SW and ML cultures and the freshly isolated hepatocytes. It was found that the expressions of DMPK-related genes of the 3-D tissue from the NP culture were globally increased more than those of the conventional 2-D tissue from the SW or ML cultures.

HCA showed that NP and SW belonged to the same cluster (Figure 2). This result indicates that the NP-cultured 3-D tissue was closer to the freshly isolated hepatocytes than was the ML-cultured 2-D tissue because it was formerly reported that the SW culture possesses

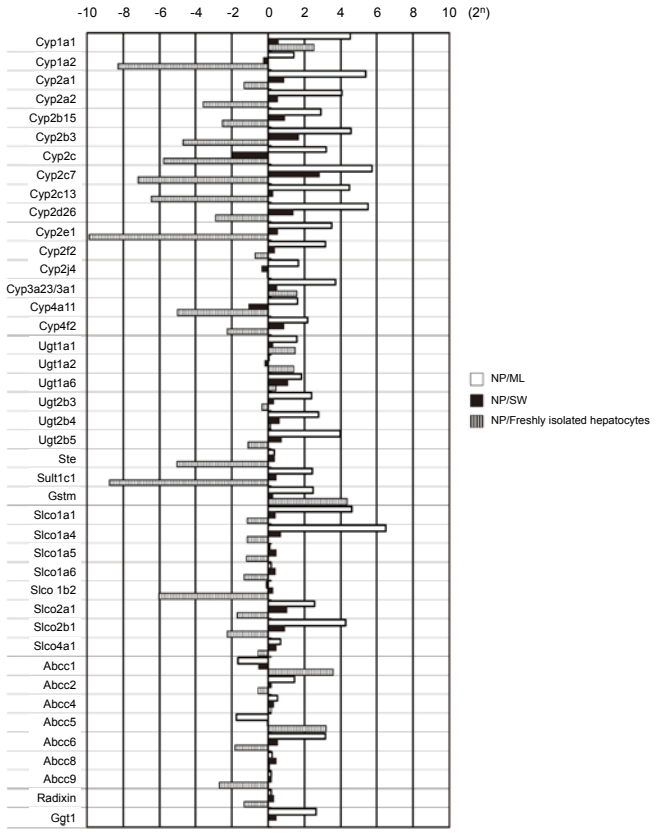

Figure 4: Quantitative comparison of phase-I (i.e., Cyp), phase II (i.e., Ugt), uptake (i.e., Slco), excretion transporter (i.e., Abcc), Radixin and Ggt1 mRNA in hepatocytes from NP culture with mRNA in hepatocytes from ML culture (NP/ML), mRNA in hepatocytes from NP culture with mRNA in hepatocytes from SW culture (NP/SW), and mRNA in hepatocytes from NP culture with mRNA in freshly isolated hepatocytes (NP/freshly isolated hepatocytes).

MAPP name	Criteria	Z score	Permute P-value
Regularion of actin cytoskeleton	2.0<[ML/NP]<=4.0	4.577	0
Alpha6-beta4-integrin	2.0<[ML/NP]<=4.0	3.032	0
Alpha6-beta4-integrin	2.0<[SW/NP]<=4.0	3.614	0.005
Focal adhesion	2.0<[SW/NP]<=4.0	2.452	0.02
Irinotecan pathway	-4.0<[ML/NP]<=2.0	3.688	0.006
Irinotecan pathway	-4.0<[SW/NP]<=2.0	3.576	0.03

Table 2: MAPP names of altered gene expression.

differentiated functions and a polarity similar to native hepatocytes than does the conventional simple monolayer culture [19]. Our finding and the indication here are consistent with the previous report that the structure and function of the 3-D spheroids formed by the NP culture was closer to that of the native tissue than that of the conventional 2-D tissue [13]. Next, PCA was carried out. The result showed that the expressional profile of the NP culture was closer to that of the freshly isolated hepatocytes than that of the SW culture (Figure 3). These results of the HCA and PCA suggest that the global expressional trend acquired from the NP culture was the closest to the freshly isolated hepatocytes under the three culture conditions conducted in this study. As the result of PCA, the freshly isolated hepatocytes and ML were plotted widely apart, and NP and SW were plotted closely between the two groups in PC1 (63.3%) (Figure 3). It is considered that PC1 reflects the difference of the culture condition. In comparison, a contributory factor of PC2, in which case the group of NP/SW and that of the freshly isolated hepatocytes/ML are plotted clearly wide apart (Figure 3), remains to be accounted for.

The expression levels of Cyp1a1 and 3a1 in the NP culture were significantly higher than that of the freshly isolated hepatocytes. The expressions of these two genes were reported to be induced by dexamethasone, a steroidal anti-inflammatory drug [39-41]. Since 255 nM of dexamethasone is included in all the culture media used in this study, we considered that the effect was due to the dexamethasone. Abcc genes constitute a family in terms of gene sequence and biological function; however, their substrates differ according to each gene. In this study, we reported that the expression trend of Abcc genes differed from one gene to another unlike the molecules such as phase-I and phase-II or uptake transporter genes. This finding is likely to be because several phase-I and -II metabolic enzymes produced a wide variety of metabolites due to the differences in culture conditions, and consequently, variations of up-regulated or down-regulated excretion transporters were observed. Glucuronic-conjugated bilirubin generated by UGT1A1 metabolic action was reported to be excreted into bile canaliculi by MRP2 that is a translation product of Abcc2 gene [31,32]. The present study showed the gene expressions of Ugt1a1 and Abcc2 were both up-regulated in the 3-D spheroids by the NP culture (Figure 4). This result suggests that the up-regulation of the conjugation enzyme occurred in conjunction with that of the excretion transporter in the 3-D NP culture. Therefore, it is proposed that the metabolic process by which hepatocytes configure the 3-D spheroids in the NP culture metabolizes more bilirubin (B) into conjugated bilirubin (B*) than does that by conventional 2-D-cultured hepatocytes (Figures 5a and 5b). Because of this, more conjugated bilirubin (B*) is speculated to be excreted by MRP2. Enhanced expression of the Abcc2 gene related to biliary excretion in conjunction with Ugt1a1 strongly indicates that the NP-cultured 3-D spheroid has the potential to fulfill a higher hepatocellular metabolic function than does 2-D tissue formed by conventional monolayer culture.

In the pathway analyses, the Irinotecan pathway, which is related to the metabolic process in hepatocytes, was activated more in the NP-cultured 3-D spheroid than in the ML- or SW-cultured 2-D tissue (Table 2). PCA showed that the gene expression profile obtained from the NP-cultured 3-D spheroids was closer to that from the freshly isolated hepatocytes than that from the SW-cultured 2-D tissue (Figure 2). These findings, along with the results of expressional analyses of DMPK-related genes (Figure 4), account for the fact that the 3-D spheroids formed by the NP culture possessed higher metabolic ability and function closer to that of the native liver, which also support our hypothesis presented in figure 5. It is considered that one reason for these findings is that the number of cell-cell adhesion sites of the 3-D spheroid is larger than that of 2-D tissue, and accordingly, the 3-D spheroid has more bile canaliculi. Consequently, hepatocytes came to possess a structural polarity and tended to recover the primary functions of the liver by establishing a 3-D structure [2,7,11].

The correlation of tissue structure and hepatic function were also presented in this study. The pathway related to cell-matrix adhesion was more activated in the ML- or SW-cultured 2-D cultures than in the NP-cultured 3-D spheroids. In other words, the number of the expressed molecules of talin of the NP culture is smaller than that of the ML culture. This speculation indicates that the growing number of cell-cell adhesion site were formed in the NP-cultured 3-D spheroid, consequently the spheroid exhibited better structure closer to an *in vivo* native environment than did the conventional 2-D culture (Figure 5). Our previous study showed the correlation between decreased expression of talin and formation of 3-D structure [13], which was consistent with the result of the present study. Moreover, the expression of radixin in the NP-cultured 3-D spherood was higher than that in ML- and SW-cultured monolayer tissue. Radixin has been reported to selectively tether MRP2 to the apical canalicular membrane [42], and is required to maintain apical canalicular membrane structure, polarity and function in hepatocytes [43]. On the basis of these findings, our result suggests that higher expression of radixin in the NP-cultured spheroid lead MRP2 to be retained on the membrane. Accordingly, more conjugated bilirubin (B*), as an example, is speculated to have been excreted (Figure 5).

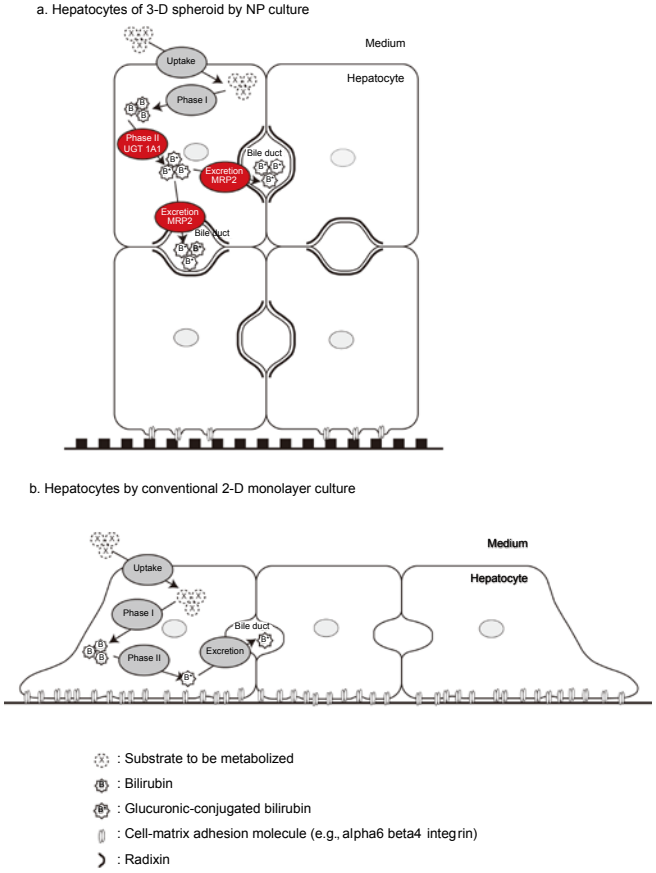

Figure 5: Proposed metabolic process of bilirubin. a: hepatocytes of the 3-D spheroids by the NP culture. b: hepatocytes of the conventional 2-D monolayer culture. Up-regulated genes are highlighted in red.

In conclusion, the DNA microarray analysis showed that the expressions of cytochrome P450, UDP-glucuronosyltransferase, and transporter genes in the NP-cultured 3-D spheroids were globally more enhanced than those in the conventional ML- or SW-cultured 2-D tissue. Comprehensive increase in the expression of the DMPK-related genes of the NP-cultured 3-D spheroids is a definitive finding toward establishing an *in vitro* drug screening method. The NP culture has potential as an alternative culturing technique for evaluating metabolism and toxicity toward the development of new drugs.

Acknowledgements

We are grateful to Dr. Yasuhiko Tabata, Shigeharu Nishiuchi, Masabumi Nemoto, and Taku Saito for their helpful comments and suggestions.

References

1. Smith NF, Raynaud FI, Workman P (2007) The application of cassette dosing for pharmacokinetic screening in small-molecule cancer drug discovery. Mol Cancer Ther 6: 428-440.
2. Elkayam T, Amitay-Shaprut S, Dvir-Ginzberg M, Harel T, Cohen S (2006) Enhancing the drug metabolism activities of C3A--a human hepatocyte cell line--by tissue engineering within alginate scaffolds. Tissue Eng 12: 1357-1368.
3. Lau YY, Chen YH, Liu TT, Li C, Cui X, et al. (2004) Evaluation of a novel in vitro Caco-2 hepatocyte hybrid system for predicting in vivo oral bioavailability. Drug Metab Dispos 32: 937-942.
4. Kola I, Landis J (2004) Can the pharmaceutical industry reduce attrition rates? Nat Rev Drug Discov 3: 711-715.
5. Roberts SA (2003) Drug metabolism and pharmacokinetics in drug discovery. Curr Opin Drug Discov Devel 6: 66-80.
6. Abu-Absi SF, Friend JR, Hansen LK, Hu WS (2002) Structural polarity and functional bile canaliculi in rat hepatocyte spheroids. Exp Cell Res 274: 56-67.
7. Hamilton GA, Westmorel C, George AE (2001) Effects of medium composition on the morphology and function of rat hepatocytes cultured as spheroids and monolayers. In Vitro Cell Dev Biol Anim 37: 656-667.
8. Koide N, Sakaguchi K, Koide Y, Asano K, Kawaguchi M, et al. (1990) Formation of multicellular spheroids composed of adult rat hepatocytes in dishes with positively charged surfaces and under other nonadherent environments. Exp Cell Res 186: 227-235.
9. Bissell DM, Stamatoglou SC, Nermut MV, Hughes RC (1986) Interactions of rat hepatocytes with type IV collagen, fibronectin and laminin matrices. Distinct matrix-controlled modes of attachment and spreading. Eur J Cell Biol 40: 72-78.
10. Bissell DM, Guzelian PS (1980) Phenotypic stability of adult rat hepatocytes in primary monolayer culture. Ann N Y Acad Sci 349: 85-98.
11. Dvir-Ginzberg M, Elkayam T, Aflalo ED, Agbaria R, Cohen S (2004) Ultrastructural and functional investigations of adult hepatocyte spheroids during in vitro cultivation. Tissue Eng 10: 1806-1817.
12. Hamamoto R, Yamada K, Kamihira M, Iijima S (1998) Differentiation and proliferation of primary rat hepatocytes cultured as spheroids. J Biochem 124: 972-979.
13. Takahashi R, Sonoda H, Tabata Y, Hisada A (2010) Formation of hepatocyte spheroids with structural polarity and functional bile canaliculi using nanopillar sheets. Tissue Eng Part A 16: 1983-1995.
14. Landry J, Bernier D, Ouellet C, Goyette R, Marceau N (1985) Spheroidal aggregate culture of rat liver cells: histotypic reorganization, biomatrix deposition, and maintenance of functional activities. J Cell Biol 101: 914-923.
15. Tong JZ, Sarrazin S, Cassio D, Gauthier F, Alvarez F (1994) Application of spheroid culture to human hepatocytes and maintenance of their differentiation. Biol Cell 81: 77-81.
16. Fukuda J, Nakazawa K (2005) Orderly arrangement of hepatocyte spheroids on a microfabricated chip. Tissue Eng 11: 1254-1262.
17. Seglen PO (1976) Preparation of isolated rat liver cells. Methods Cell Biol 13: 29-83.
18. Kreamer BL, Staecker JL, Sawada N, Sattler GL, Hsia MT, et al. (1986) Use of a low-speed, iso-density percoll centrifugation method to increase the viability of isolated rat hepatocyte preparations. In Vitro Cell Dev Biol 22: 201-211.
19. Caron JM (1990) Induction of albumin gene transcription in hepatocytes by extracellular matrix proteins. Mol Cell Biol 10: 1239-1243.
20. Dunn JC, Yarmush ML, Koebe HG, Tompkins RG (1989) Hepatocyte function and extracellular matrix geometry: long-term culture in a sandwich configuration. FASEB J 3: 174-177.
21. Tanaka H, Shimazawa M, Kimura M, Takata M, Tsuruma K, et al. (2012) The potential of GPNMB as novel neuroprotective factor in amyotrophic lateral sclerosis. Sci Rep 2: 573.
22. Mathijs K, Brauers KJ, Jennen DG, Lizarraga D, Kleinjans JC, et al. (2010) Gene expression profiling in primary mouse hepatocytes discriminates true from false-positive genotoxic compounds. Mutagenesis 25: 561-568.
23. de Haan JR, Wehrens R, Bauerschmidt S, Piek E, van Schaik RC, et al. (2007) Interpretation of ANOVA models for microarray data using PCA. Bioinformatics 23: 184-190.
24. Nelson DR, Koymans L, Kamataki T, Stegeman JJ, Feyereisen R, et al. (1996) P450 superfamily: update on new sequences, gene mapping, accession numbers and nomenclature. Pharmacogenetics 6: 1-42.
25. Tukey RH, Strassburg CP (2000) Human UDP-glucuronosyltransferases: metabolism, expression, and disease. Annu Rev Pharmacol Toxicol 40: 581-616.
26. Dawson PA, Lan T, Rao A (2009) Bile acid transporters. J Lipid Res 50: 2340-2357.
27. Williams JA, Hyland R, Jones BC, Smith DA, Hurst S, et al. (2004) Drug-drug interactions for UDP-glucuronosyltransferase substrates: a pharmacokinetic explanation for typically observed low exposure (AUCi/AUC) ratios. Drug Metab Dispos 32: 1201-1208.
28. Nakakariya M, Ono M, Amano N, Moriwaki T, Maeda K, et al. (2012) In vivo biliary clearance should be predicted by intrinsic biliary clearance in sandwich-cultured hepatocytes. Drug Metab Dispos 40: 602-609.
29. Watanabe T, Kusuhara H, Maeda K, Kanamaru H, Saito Y, et al. (2010) Investigation of the rate-determining process in the hepatic elimination of HMG-CoA reductase inhibitors in rats and humans. Drug Metab Dispos 38: 215-222.
30. Jigorel E, Le Vee M, Boursier-Neyret C, Bertrand M, Fardel O (2005) Functional expression of sinusoidal drug transporters in primary human and rat hepatocytes. Drug Metab Dispos 33: 1418-1422.
31. Suzuki H, Sugiyama Y (2002) Single nucleotide polymorphisms in multidrug resistance associated protein 2 (MRP2/ABCC2): its impact on drug disposition. Adv Drug Deliv Rev 54: 1311-1331.
32. Nies AT, Keppler D (2007) The apical conjugate efflux pump ABCC2 (MRP2). Pflugers Arch 453: 643-659.
33. Zhang P, Tian X, Chandra P, Brouwer KL (2005) Role of glycosylation in trafficking of Mrp2 in sandwich-cultured rat hepatocytes. Mol Pharmacol 67: 1334-1341.
34. Leier I, Jedlitschky G, Buchholz U, Cole SP, Deeley RG, et al. (1994) The MRP gene encodes an ATP-dependent export pump for leukotriene C4 and structurally related conjugates. J Biol Chem 269: 27807-27810.
35. MÃ¼ller M, Meijer C, Zaman GJ, Borst P, Scheper RJ, et al. (1994) Overexpression of the gene encoding the multidrug resistance-associated protein results in increased ATP-dependent glutathione S-conjugate transport. Proc Natl Acad Sci U S A 91: 13033-13037.
36. Jedlitschky G, Burchell B, Keppler D (2000) The multidrug resistance protein 5 functions as an ATP-dependent export pump for cyclic nucleotides. J Biol Chem 275: 30069-30074.
37. NemesÃ¡nszky E, Lott JA (1985) Gamma-glutamyltransferase and its isoenzymes: progress and problems. Clin Chem 31: 797-803.
38. Clark SP, Davis MA, Ryan TP, Searfoss GH, Hooser SB (2007) Hepatic gene expression changes in mice associated with prolonged sublethal microcystin exposure. Toxicol Pathol 35: 594-605.
39. Backman JT, Olkkola KT, Neuvonen PJ (1996) Rifampin drastically reduces plasma concentrations and effects of oral midazolam. Clin Pharmacol Ther 59: 7-13.
40. Pichard L, Fabre I, Daujat M, Domergue J, Joyeux H, et al. (1992) Effect of corticosteroids on the expression of cytochromes P450 and on cyclosporin A

oxidase activity in primary cultures of human hepatocytes. Mol Pharmacol 41: 1047-1055.

41. Lai KP, Wong MH, Wong CK (2004) Modulation of AhR-mediated CYP1A1 mRNA and EROD activities by 17beta-estradiol and dexamethasone in TCDD-induced H411E cells. Toxicol Sci 78: 41-49.

42. Kikuchi S, Hata M, Fukumoto K, Yamane Y, Matsui T, et al. (2002) Radixin deficiency causes conjugated hyperbilirubinemia with loss of Mrp2 from bile canalicular membranes. Nat Genet 31: 320-325.

43. Wang W, Soroka CJ, Mennone A, Rahner C, Harry K, et al. (2006) Radixin is required to maintain apical canalicular membrane structure and function in rat hepatocytes. Gastroenterology 131: 878-884.